Measurements of branching fractions of $D^0 \to K^-3\pi^+2\pi^-$, $D^0 \to K^-2\pi^+\pi^-2\pi^0$, and $D^+ \to K^-3\pi^+\pi^-\pi^0$

M. Ablikim *et al.*[*]
(BESIII Collaboration)

(Received 27 April 2025; accepted 19 June 2025; published 2 July 2025)

Utilizing 7.9 fb^{-1} of e^+e^- collision data taken with the BESIII detector at the center-of-mass energy of 3.773 GeV, we report the measurements of absolute branching fractions of the hadronic decays $D^0 \to K^-3\pi^+2\pi^-$, $D^0 \to K^-2\pi^+\pi^-2\pi^0$ and $D^+ \to K^-3\pi^+\pi^-\pi^0$. The $D^0 \to K^-3\pi^+2\pi^-$ decay is measured with improved precision, while the latter two decays are observed with statistical significance higher than 5σ for the first time. The absolute branching fractions of these decays are determined to be $\mathcal{B}(D^0 \to K^-3\pi^+2\pi^-) = (1.35 \pm 0.23 \pm 0.08) \times 10^{-4}$, $\mathcal{B}(D^0 \to K^-2\pi^+\pi^-2\pi^0) = (19.0 \pm 1.1 \pm 1.5) \times 10^{-4}$, and $\mathcal{B}(D^+ \to K^-3\pi^+\pi^-\pi^0) = (6.57 \pm 0.69 \pm 0.33) \times 10^{-4}$, where the first uncertainties are statistical and the second systematic.

DOI: 10.1103/nyy9-318k

I. INTRODUCTION

Experimental measurements of hadronic D decays are important for studies of CP violation, $D^0 - \bar{D}^0$ mixing, and flavor SU(3) symmetry breaking effects in the charm sector [1–5]. Precise and comprehensive measurements of the absolute branching fractions (BFs) of hadronic decays of D mesons containing three charged pions are valuable inputs for understanding important backgrounds in studies of $B \to D^{*-}\tau^+\nu_\tau$ decays, where enticing hints of lepton flavor universality violation are observed [6,7].

The measured BFs of the inclusive decays $D^{0(+)} \to \pi^+\pi^+\pi^-X$ [8] indicate that there is some room for unmeasured $D^{0(+)}$ decays containing three charged pions, which are $(1.55 \pm 0.50)\%$ and $(0.51 \pm 0.57)\%$ for D^0 and D^+ decays, respectively. Certain Cabbibo-favored multibody hadronic $D^{0(+)}$ decays containing one kaon and multiple pions, are promising, as proposed by Ref. [9]. Much progress has been made recently in experimental studies of $D^{0(+)}$ decays containing one kaon along with one to four pions [10]. However, the experimental knowledge of the hadronic $D^{0(+)}$ decays containing one kaon and five pions is very poor, mainly due to limited data sample and small BFs [10]. Previously, only the FOCUS Collaboration reported $\mathcal{B}(D^0 \to K^-3\pi^+2\pi^-) = (2.2 \pm 0.6) \times 10^{-4}$ [11] based on a relative branching ratio. The large e^+e^- collision data sample taken at the $\psi(3770)$ peak with the BESIII detector allows for measuring the absolute BFs of these six-body hadronic decays.

In this paper, we report measurements of the absolute BFs of the hadronic decays $D^0 \to K^-3\pi^+2\pi^-$, $D^0 \to K^-2\pi^+\pi^-2\pi^0$ and $D^+ \to K^-3\pi^+\pi^-\pi^0$, by analyzing the e^+e^- collision data corresponding to an integrated luminosity of 7.9 fb^{-1} [12–14] collected with the BESIII detector at the center-of-mass energy $E_{\rm cm} = 3.773$ GeV. Throughout this paper, charge conjugation is always implied, and $D(\bar{D})$ denotes $D^+, D^0(\bar{D}^0, D^-)$ mesons.

II. BESIII DETECTOR AND MONTE CARLO SIMULATION

The BESIII detector [15] records symmetric e^+e^- collisions provided by the BEPCII storage ring [16] in the center-of-mass energy range from 1.84 to 4.95 GeV, with a peak luminosity of 1.1×10^{33} cm^{-2} s^{-1} achieved at $E_{\rm cm} = 3.773$ GeV. The cylindrical core of the BESIII detector covers 93% of the full solid angle and consists of a helium-based multilayer drift chamber (MDC), a time-of-flight system (TOF), and a CsI(Tl) electromagnetic calorimeter (EMC), which are all enclosed in a superconducting solenoidal magnet providing a 1.0 T magnetic field. The solenoid is supported by an octagonal flux-return yoke with resistive plate counter muon identification modules interleaved with steel. The charged-particle momentum resolution at 1 GeV/c is 0.5%, and the dE/dx resolution is 6% for electrons from Bhabha scattering. The EMC measures photon energies with a resolution of 2.5% (5%) at 1 GeV in the barrel (end-cap) region. The time resolution in the plastic scintillator TOF barrel region is 68 ps, while that in the end-cap region was 110 ps.

[*]Full author list given at the end of the article.

The end-cap TOF system was upgraded in 2015 using multigap resistive plate chamber technology, providing a time resolution of 60 ps, which benefits 63% of the data used in this analysis [17].

Monte Carlo (MC) simulated data samples produced with a GEANT4-based [18] software package, which includes the geometric description of the BESIII detector and the detector response, are used to determine detection efficiencies and to estimate backgrounds. The simulation models the beam energy spread and initial state radiation (ISR) in the e^+e^- annihilations with the generator KKMC [19]. The inclusive MC sample includes the production of $D\bar{D}$ pairs (with quantum coherence for the $D^0, \bar{D}^0$ channels), the non-$D\bar{D}$ decays of the $\psi(3770)$, the ISR production of the J/ψ and $\psi(3686)$ states, and the continuum processes incorporated in KKMC [19]. All particle decays are modeled with EVTGEN [20] using BFs either taken from the Particle Data Group [10], when available, or otherwise estimated with LUNDCHARM [21]. Final state radiation from charged final state particles is incorporated using the PHOTOS package [22].

III. MEASUREMENT METHOD

In e^+e^- collisions at $E_{\rm cm} = 3.773$ GeV, the $D^0\bar{D}^0$ or D^+D^- pairs are produced without any additional hadrons. This property offers an ideal platform to measure the absolute BFs of the hadronic D decays by using the double-tag (DT) method [23]. The single-tag (ST) $\bar{D}^0$ mesons are reconstructed from three hadronic decays $\bar{D}^0 \to K^+\pi^-$, $K^+\pi^-\pi^0$, $K^+\pi^-\pi^-\pi^+$, and the ST D^- mesons are reconstructed from six hadronic decays $D^- \to K^+\pi^-\pi^-$, $K^0_S\pi^-$, $K^+\pi^-\pi^-\pi^0$, $K^0_S\pi^-\pi^0$, $K^0_S\pi^+\pi^-\pi^-$, and $K^+K^-\pi^-$. Then DT candidates are formed by selecting signal decays in the recoiling side against the $\bar{D}$ mesons. The BF of the signal decay can be determined as

$$\mathcal{B}_{\rm sig} = N_{\rm DT}/(N^{\rm tot}_{\rm ST}\epsilon_{\rm sig}), \tag{1}$$

where $N^{\rm tot}_{\rm ST}$ is the yield of ST $\bar{D}$ mesons summed over all tag modes, $N_{\rm DT}$ is the yield of DT events, and $\epsilon_{\rm sig}$ is the efficiency of detecting the signal D decay, averaged over all tag modes, given by

$$\epsilon_{\rm sig} = \sum_i (N^i_{\rm ST}\epsilon^i_{\rm DT}/\epsilon^i_{\rm ST})/N^{\rm tot}_{\rm ST}, \tag{2}$$

where $\epsilon^i_{\rm ST}$ and $\epsilon^i_{\rm DT}$ are the efficiencies of detecting ST and DT candidates in the tag mode i, respectively.

IV. EVENT SELECTION

All charged tracks, except those from K^0_S decays, are required to satisfy $V_{xy} < 1$ cm, $|V_z| < 10$ cm, where V_{xy} and V_z are the distances of closest approach to the interaction point along the beam direction and in the plane perpendicular to the beam direction, respectively. We also require $|\cos\theta| < 0.93$, where θ is the polar angle with respect to the symmetry axis of the MDC. We perform particle identification (PID) on charged tracks with combined dE/dx and TOF information, using the calculated confidence levels [24] for the pion and kaon hypotheses, CL_π and CL_K. Tracks with $CL_K > CL_\pi$ and $CL_\pi > CL_K$ are assigned as kaon and pion candidates, respectively.

The K^0_S candidates are reconstructed via $K^0_S \to \pi^+\pi^-$ decays. Two oppositely charged tracks are required to satisfy $|V_z| < 20$ cm and $|\cos\theta| < 0.93$, and they are assumed to be pions with no PID. The accepted $\pi^+\pi^-$ pairs are then constrained to originate from a common vertex and their invariant mass is required to be within $(0.487, 0.511)$ GeV/c^2, corresponding to approximately three times the fitted resolution around the known K^0 mass [10]. The decay length of each K^0_S candidate must be at least twice the vertex resolution from the interaction point. The four-vector from the vertex fit is used for later kinematics.

The π^0 candidates are reconstructed via $\pi^0 \to \gamma\gamma$ decays. Each photon candidate is selected from EMC shower start time within 700 ns of the event start time and a minimal deposited energy of more than 25 MeV in the barrel region ($|\cos\theta| < 0.80$) or 50 MeV in the end-cap region ($0.86 < |\cos\theta| < 0.92$). The energy deposited in the neighboring TOF counters is included to improve the reconstruction efficiency and energy resolution. The minimum opening angle between the shower and the nearest charged track must be larger than 10°. The $\gamma\gamma$ combinations with invariant masses in the range of $(0.115, 0.150)$ GeV/c^2 are retained as π^0 candidates. To improve the resolution, a kinematic fit is performed on the selected photon pair, constraining the $\gamma\gamma$ invariant mass to the known π^0 mass [10] and the constrained four-vector is used for later kinematics.

For $\bar{D}^0 \to K^+\pi^-$ candidates, backgrounds from cosmic rays and Bhabha events are removed with the following requirements. First, the two charged tracks must have a TOF time difference of less than 5 ns and they must not be consistent with being a muon pair or an electron-positron pair. Second, there must be at least one EMC shower with an energy larger than 50 MeV or at least one additional good (i.e., passing the previous selections) charged track detected in the MDC [25].

V. YIELDS OF SINGLE-TAG $\bar{D}$ MESONS

We use the same method to obtain the ST yields and ST efficiencies as in Ref. [26]. To distinguish the tagged $\bar{D}$ mesons from combinatorial backgrounds, we define two kinematic variables, e.g., energy difference

$$\Delta E_{\rm tag} \equiv E_{\rm tag} - E_{\rm b}, \tag{3}$$

and beam-constrained mass

TABLE I. The ΔE^i requirements, the ST $\bar{D}$ yields in data, $N^i_{\rm ST}$, and the ST efficiencies, $\epsilon^i_{\rm ST}$, for each tag mode, where the uncertainties are statistical only.

Tag mode	ΔE^i (GeV)	$N^i_{\rm ST}(\times 10^3)$	$\epsilon^i_{\rm ST}(\%)$
$\bar{D}^0 \to K^+\pi^-$	$(-0.027, 0.027)$	1482.8 ± 1.3	66.89 ± 0.01
$\bar{D}^0 \to K^+\pi^-\pi^0$	$(-0.062, 0.049)$	3118.2 ± 2.1	37.68 ± 0.01
$\bar{D}^0 \to K^+\pi^-\pi^-\pi^+$	$(-0.026, 0.024)$	1997.9 ± 1.6	41.88 ± 0.01
$D^- \to K^+\pi^-\pi^-$	$(-0.025, 0.024)$	2215.3 ± 1.6	52.44 ± 0.01
$D^- \to K^0_S\pi^-$	$(-0.025, 0.026)$	256.0 ± 0.5	51.89 ± 0.02
$D^- \to K^+\pi^-\pi^-\pi^0$	$(-0.057, 0.046)$	735.4 ± 1.2	27.19 ± 0.01
$D^- \to K^0_S\pi^-\pi^0$	$(-0.062, 0.049)$	590.4 ± 1.0	27.57 ± 0.01
$D^- \to K^0_S\pi^+\pi^-\pi^-$	$(-0.028, 0.027)$	307.7 ± 0.7	29.68 ± 0.01
$D^- \to K^+K^-\pi^-$	$(-0.024, 0.023)$	191.8 ± 0.5	42.05 ± 0.02

$$M^{\rm tag}_{\rm BC} \equiv \sqrt{E^2_{\rm b} - |\vec{p}_{\rm tag}|^2}, \tag{4}$$

where $E_{\rm b}$ is the beam energy, and $\vec{p}_{\rm tag}$ and $E_{\rm tag}$ are the momentum and energy of the tagged $\bar{D}$ candidate in the rest frame of e^+e^- system, respectively. The ΔE^i requirements for different tag modes are listed in Table I. For each tag mode, if there are multiple candidates in an event, we only retain the one giving the minimum value of $|\Delta E_{\rm tag}|$ [26].

To extract the yield of ST $\bar{D}$ mesons for each tag mode, a binned maximum-likelihood fit is performed on the $M^{\rm tag}_{\rm BC}$ distribution of the accepted candidates. In the fit, the $\bar{D}$ signal is described with an MC-simulated shape convolved with a double-Gaussian function to take into account the difference in resolution between data and MC simulation. The combinatorial background is described by an ARGUS function [27]. The results of the fits to the $M_{\rm BC}$ distributions of different tag modes are shown in Fig. 1. The ST $\bar{D}$ yields in data and ST efficiencies for the different tag modes are listed in Table I. Summing over all tag modes gives the total yields of ST $\bar{D}^0$ and D^- mesons to be $(6599.0 \pm 2.9_{\rm stat}) \times 10^3$ and $(4296.6 \pm 2.4_{\rm stat}) \times 10^3$, respectively.

VI. YIELDS OF DOUBLE-TAG EVENTS

Candidates for signal D decays are selected using the remaining tracks and showers not used for reconstructing the tag side $\bar{D}$ (ST). The charged D signal decay must have charge opposite to that of the tag side; while for the neutral D signal decays, the charge of the kaon on the signal side must be opposite to that on the tag side. For all three signal decays, to suppress backgrounds with $\pi^+\pi^-$ produced from $K^0_S \to \pi^+\pi^-$ decays, the $\pi^+\pi^-$ invariant masses are required to be outside the range of $(0.468, 0.528)$ GeV/c^2. For $D^0 \to K^-2\pi^+\pi^-2\pi^0$, to suppress backgrounds from $D^0 \to K^-2\pi^+\pi^- K^0_S(\to\pi^0\pi^0)$, the $\pi^0\pi^0$ invariant masses are

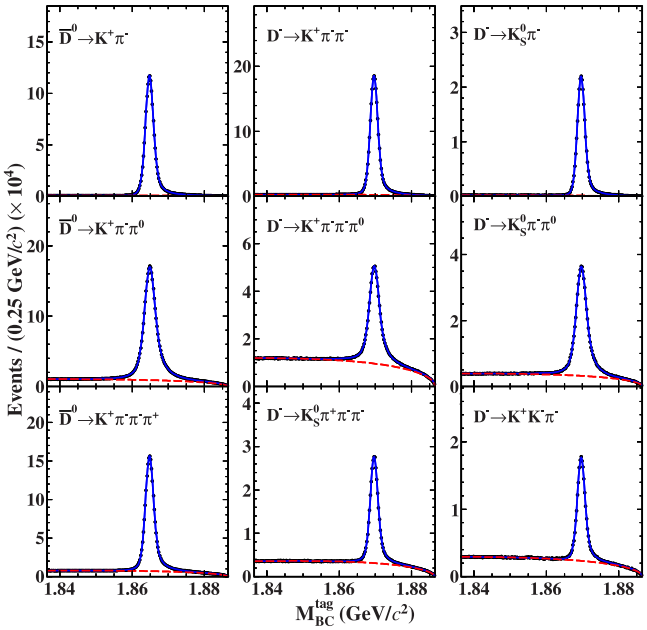

FIG. 1. Fits to the $M^{\rm tag}_{\rm BC}$ distributions of the $\bar{D}^0$ (left column) and D^- (middle and right columns) ST candidates. The points with error bars are data, the solid blue curves are the fit results, and the dashed red curves are the fitted background components.

required to be outside the range of $(0.448, 0.548)$ GeV/c^2. We note that various narrow hadronic resonances (e.g., $\eta, \eta', \omega, \phi$) potentially present in the final state are not removed.

The signal D mesons are identified using the energy difference $\Delta E_{\rm sig}$ and the beam-constrained mass $M^{\rm sig}_{\rm BC}$, which are calculated with Eqs. (3) and (4), respectively, by replacing "sig" with "tag.". For each signal D decay, if there are multiple candidates in an event, only the one with the smallest $|\Delta E_{\rm sig}|$ is kept for further analysis. The signal D decays are required to satisfy mode-dependent $\Delta E_{\rm sig}$ requirements, as shown in the second column of Table II.

Figure 2 shows the $M^{\rm tag}_{\rm BC}$ versus $M^{\rm sig}_{\rm BC}$ distribution of the accepted DT candidates in data. The signal events concentrate around $M^{\rm tag}_{\rm BC} = M^{\rm sig}_{\rm BC} = M_D$, where M_D is the known D mass [10]. The events distributed along the lines near $M^{\rm tag}_{\rm BC} = M_D$ or $M^{\rm sig}_{\rm BC} = M_D$, defined as BKGI, are mainly from a correctly reconstructed $D(\bar{D})$ combined with an incorrectly reconstructed $\bar{D}(D)$. The events smeared along the diagonal line, defined as BKGII, referred to as ISR, are mainly from the $e^+e^- \to q\bar{q}$ processes and incorrectly reconstructed $D\bar{D}$. The events dispersed across the whole plane, defined as BKGIII, are mainly from incorrectly reconstructed D and $\bar{D}$.

For each signal D decay, the yield of DT events, $N_{\rm DT}$, is obtained from a two-dimensional (2D) unbinned maximum-likelihood fit [28] to the $M^{\rm tag}_{\rm BC}$ versus $M^{\rm sig}_{\rm BC}$ distribution of the accepted candidates. In the fit, the probability density

TABLE II. The $\Delta E_{\rm sig}$ requirements, the fitted DT yields ($N_{\rm DT}$), the signal efficiencies ($\epsilon_{\rm sig}$), and the obtained BFs ($\mathcal{B}_{\rm sig}$) for each signal decay, where the first and second uncertainties of $\mathcal{B}_{\rm sig}$ are statistical and systematic, respectively, while the uncertainties of $N_{\rm DT}$ and $\epsilon_{\rm sig}$ are statistical only.

Signal decay	$\Delta E_{\rm sig}$ (GeV)	$N_{\rm DT}$	$\epsilon_{\rm sig}$ (%)	$\mathcal{B}_{\rm sig}$ ($\times 10^{-4}$)
$D^0 \to K^-3\pi^+2\pi^-$	$(-0.031, 0.028)$	64 ± 11	7.20 ± 0.19	$1.35 \pm 0.23 \pm 0.08$
$D^0 \to K^-2\pi^+\pi^-2\pi^0$	$(-0.042, 0.032)$	441 ± 26	3.61 ± 0.14	$19.0 \pm 1.1 \pm 1.5$
$D^+ \to K^-3\pi^+\pi^-\pi^0$	$(-0.036, 0.030)$	157 ± 17	5.68 ± 0.19	$6.57 \pm 0.69 \pm 0.33$

functions (PDFs) of signal, BKGI, BKGII, and BKGIII are constructed as

(i) Signal: $a(x, y)$,
(ii) BKGI: $b(x)c_y(y; E_{\rm b}, \xi_y) + b(y)c_x(x; E_{\rm b}, \xi_x)$,
(iii) BKGII: $c_z(z; \sqrt{2}E_{\rm b}, \xi_z), g(k)$,
(iv) BKGIII: $c_x(x; E_{\rm b}, \xi_x)c_y(y; E_{\rm b}, \xi_y)$,

respectively. Here, $x = M_{\rm BC}^{\rm sig}$, $y = M_{\rm BC}^{\rm tag}$, $z = (x + y)/\sqrt{2}$, and $k = (x - y)/\sqrt{2}$. The PDFs of signal $a(x, y)$, $b(x)$, and $b(y)$ are taken from the corresponding MC-simulated shapes and $c_f(f; E_{\rm end}, \xi_f)$ is the ARGUS function defined as $A_f f(1 - \frac{f^2}{E_{\rm b}^2})^{0.5} e^{\xi_f(1-(f/E_{\rm b})^2)}$, where f denotes x, y, or z; $E_{\rm b}$ is fixed at 1.8865 GeV, A_f is a normalization factor; and ξ_f is a fit parameter. The signal shape $a(x, y)$ is convolved with a 2D Gaussian function. The PDF $g(k)$ is a Gaussian function with mean of zero and standard deviation parametrized by $\sigma_k = \sigma_0(\sqrt{2}E_{\rm b}/c^2 - k)^p$, where σ_0 and p are fit parameters. For each signal decay, the statistical significance is greater than 5σ, as calculated from the maximum likelihoods with and without the signal component in the fit and accounting for the change in the number of degrees of freedom.

Figure 3 shows the $M_{\rm BC}^{\rm tag}$ and $M_{\rm BC}^{\rm sig}$ projections of the 2D fits to the data. From these fits, we obtain the DT yields of each signal D decay; these results are listed in Table II.

The DT efficiencies are estimated based on MC simulation. To account for the effect of intermediate resonance structures on the efficiency, each of these decays is modeled by a corresponding mixed-signal MC sample, in which the dominant decay modes containing resonances of η, ω, and $K^*(892)$ are mixed with the phase-space signal MC

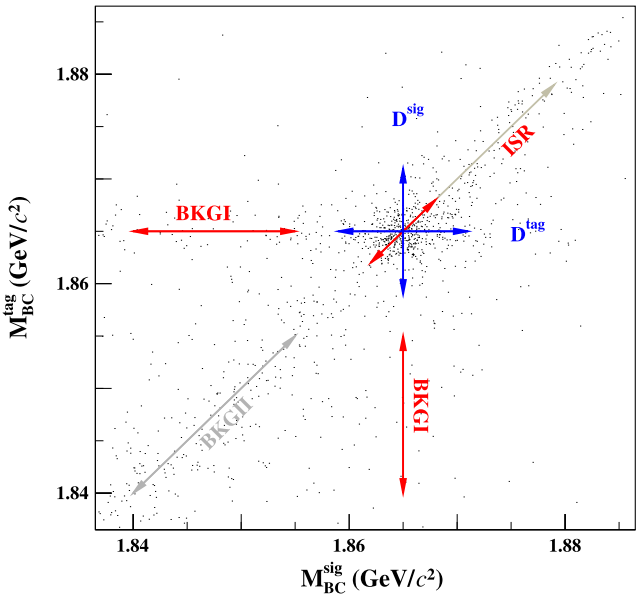

FIG. 2. The distribution of $M_{\rm BC}^{\rm tag}$ versus $M_{\rm BC}^{\rm sig}$ of the candidates for $D^0 \to K^-2\pi^+\pi^-2\pi^0$ in data, which have been summed over all $\bar{D}^0$ tag modes. Here, $D^{\rm sig}$ and $D^{\rm tag}$ denote the bands from correctly reconstructed signals, with $M_{\rm BC}^{\rm sig} = M_D$, and correctly reconstructed tags, with $M_{\rm BC}^{\rm tag} = M_D$, respectively. Backgrounds are discussed in the main text.

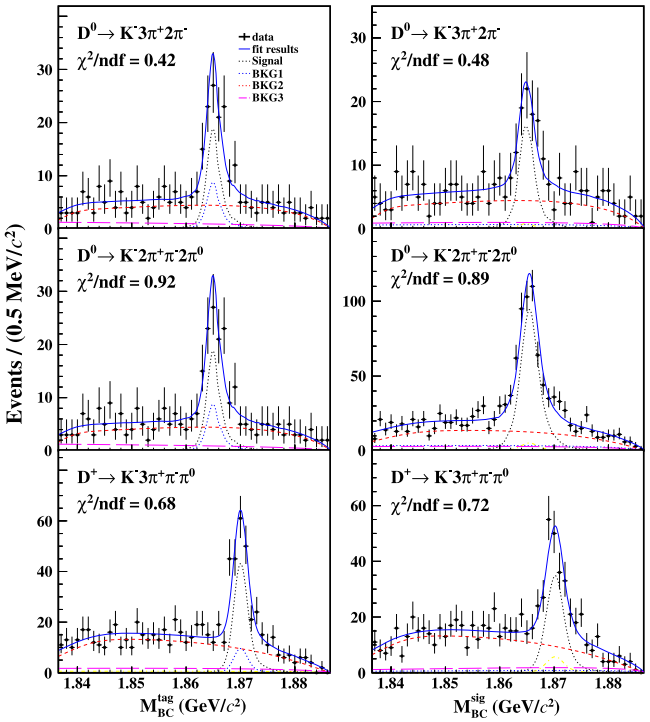

FIG. 3. Projections of the 2D fits to the distributions of (left) $M_{\rm BC}^{\rm tag}$ and (right) $M_{\rm BC}^{\rm sig}$. The points with error bars are data. The solid blue, dotted black, dot-dashed blue, dot-long-dashed red, long-dashed magenta and dashed green curves denote the overall fit results, signal, BKGI, BKGII, BKGIII, and peaking background components (see text), respectively.

samples. The mixing ratios are determined by examining the corresponding invariant mass and momentum distributions. We generate mixed signal MC samples to determine the efficiencies according to the mixing ratios. For the decay $D^0 \to K^-2\pi^+\pi^-2\pi^0$, the mixing ratio of the components $D^0 \to K^-\pi^+\pi^0\omega, K^-\pi^+\pi^0\eta, K^{*0}(892)\pi^+\pi^0\pi^-\pi^0$, $K^-2\pi^+\pi^-2\pi^0$ is 41:36:16:7. For the decay $D^+ \to K^-3\pi^+\pi^-\pi^0$, the mixing ratio of the components $D^+ \to K^{*0}(892)\pi^+\omega, K^-\pi^+\pi^+\eta, K^-3\pi^+\pi^-\pi^0$ is 54:31:15. Figures 4–6 show the distributions of momenta and cosines of polar angles of daughter particles, the invariant masses of two-body or three-body particle combinations of the accepted candidates for $D^0 \to K^-3\pi^+2\pi^-$, $D^0 \to K^-2\pi^+\pi^-2\pi^0$ and $D^+ \to K^-3\pi^+\pi^-\pi^0$ between data and MC simulations. Good consistency between data and MC simulation ensures the reliability of the signal efficiencies, provided that the efficiencies across the variables are fairly uniform and there is no large resonant signal appearing in areas of very low efficiency.

The $\Delta E_{\rm sig}$ requirements, the fitted DT yields ($N_{\rm DT}$), the signal efficiencies ($\epsilon_{\rm sig}$), and the obtained BFs ($\mathcal{B}_{\rm sig}$) for each signal decay are summarized in Table II.

VII. SYSTEMATIC UNCERTAINTIES

In the measurements of the BFs using Eq. (1), all uncertainties associated with the selection of the tag side cancel. Other uncancelled systematic uncertainties in the BF measurements are discussed below and are stated relative to the measured BFs.

The systematic uncertainties in the total yields of ST $\bar{D}$ mesons due to the fits to the $M_{\rm BC}^{\rm tag}$ distributions are estimated to be 0.3% for the ST $\bar{D}^0$ and D^- [26].

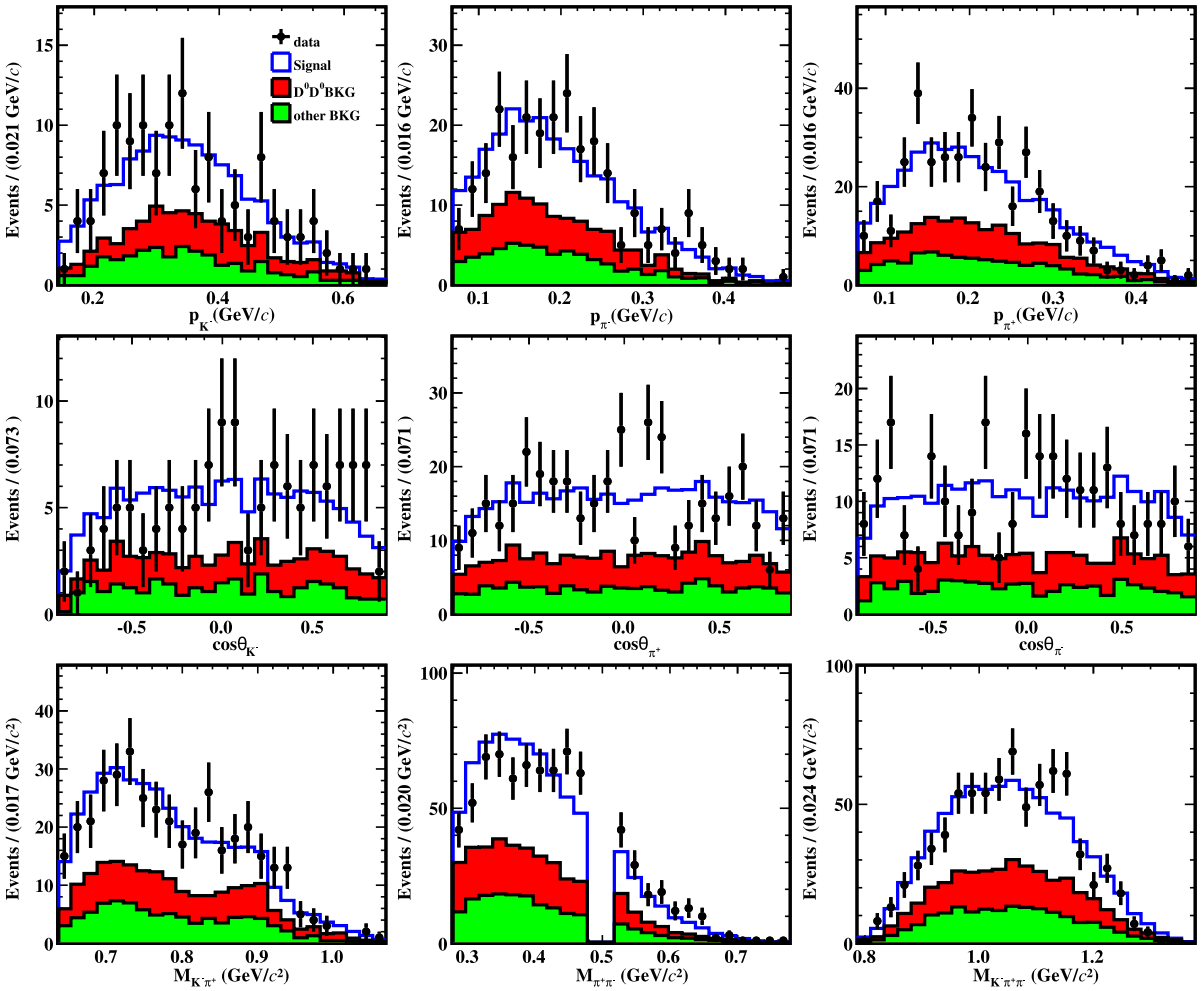

FIG. 4. Comparisons of the distributions of momenta and cosines of polar angles of daughter particles, the invariant masses of two-body or three-body particle combinations of the accepted candidates for $D^0 \to K^-3\pi^+2\pi^-$ between data (dots with error bars) and the total MC simulation (blue histogram). This total MC histogram is the sum of the signal MC events (white histogram) plus the MC-simulated backgrounds from the inclusive MC samples (red and green histograms). Events here satisfy the additional requirements of $|M_{\rm BC}^{\rm tag} - 1.865| < 0.005$ GeV/c^2 and $|M_{\rm BC}^{\rm sig} - 1.865| < 0.005$ GeV/c^2 and there are three entries for π^+ and two entries for π^- per event.

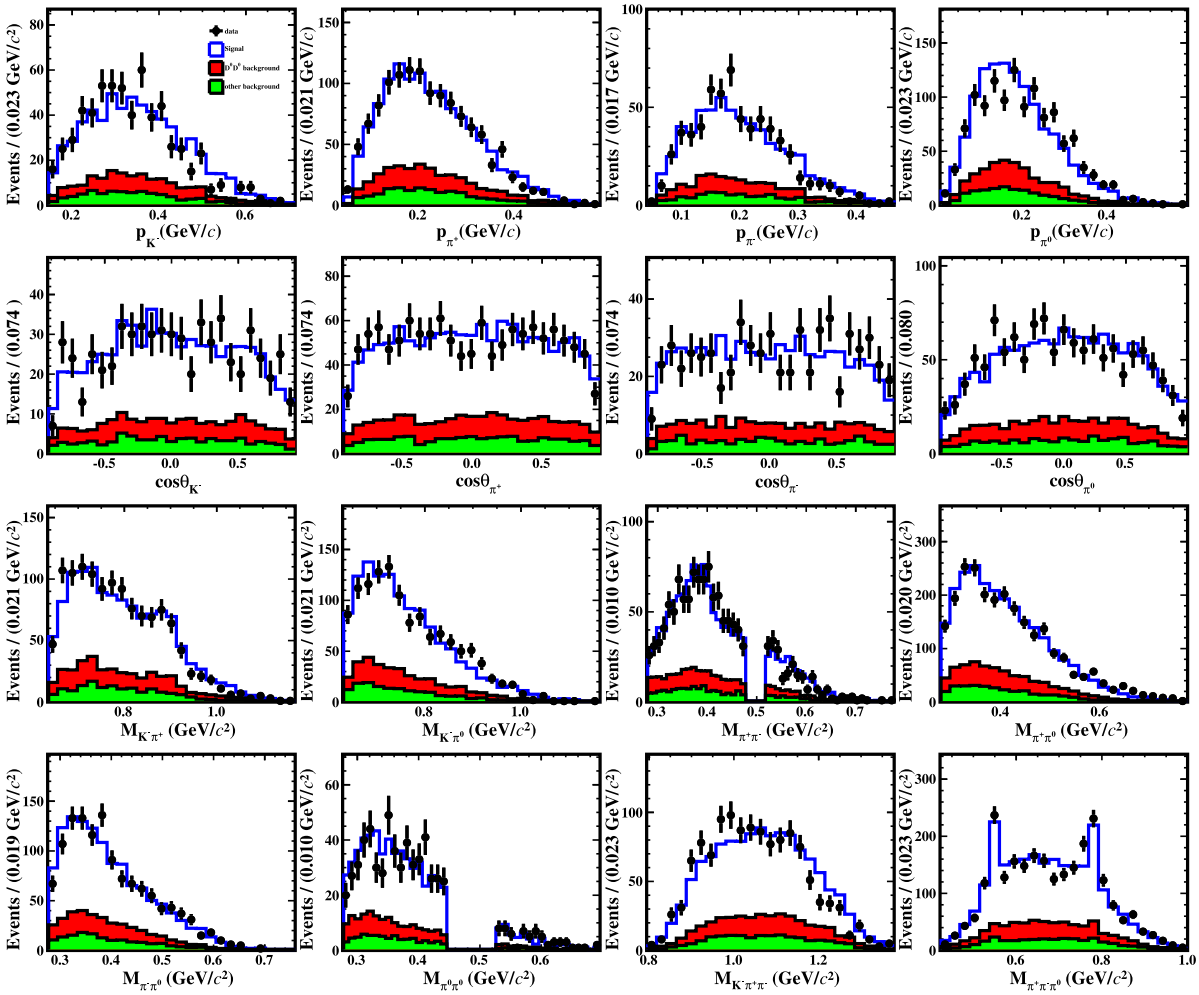

FIG. 5. Comparisons of the distributions of momenta and cosines of polar angles of daughter particles, and the invariant masses of two-body or three-body particle combinations of the accepted candidates for $D^0 \to K^-2\pi^+\pi^-2\pi^0$ between data (dots with error bars) and the total MC simulation (blue histogram). This total MC histogram is the sum of the signal MC events (white histogram) plus the MC-simulated backgrounds from the inclusive MC samples (red and green histograms). Events here satisfy the additional requirements of $|M_{\rm BC}^{\rm tag} - 1.865| < 0.005$ GeV/c^2 and $|M_{\rm BC}^{\rm sig} - 1.865| < 0.005$ GeV/c^2 and there are two entries for π^+ and two entries for π^0 per event.

The systematic uncertainties in tracking or PID of charged tracks are assigned as 0.5% per $K^\pm$ or $\pi^\pm$, by using the DT hadronic events with D decaying into $K^-\pi^+$, $K^-\pi^+\pi^+\pi^-$, $K^-\pi^+\pi^+$, and $\bar{D}$ decaying into their conjugated modes, in which a $K^\pm$ or $\pi^\pm$ is missed, as control samples [26].

The systematic uncertainty due to π^0 reconstruction is estimated to be 2.0% per π^0, by analyzing the DT hadronic events of $\bar{D}^0 \to K^+\pi^-\pi^0$ and $\bar{D}^0 \to K_S^0\pi^0$ tagged by either $D^0 \to K^-\pi^+$ or $D^0 \to K^-\pi^+\pi^+\pi^-$.

The systematic uncertainties of the $\Delta E_{\rm sig}$ requirement are assigned by using the control samples of $D^0 \to K^-\pi^+\pi^+\pi^-$, $D^0 \to K^-\pi^+\pi^0\pi^0$ and $D^+ \to K^-\pi^+\pi^+\pi^0$. The differences of the signal efficiencies are taken as the systematic uncertainties, 1.5%, 3.6%, and 1.6% for $D^0 \to K^-3\pi^+2\pi^-$, $D^0 \to K^-2\pi^+\pi^-2\pi^0$, and $D^+ \to K^-3\pi^+\pi^-\pi^0$, respectively.

The systematic uncertainty due to the K_S^0 rejection is studied with the control samples of $D^+ \to K_S^0 e^+\nu_e$ and $D^0 \to K_S^0\pi^+\pi^+\pi^-\pi^-$. The fitted K_S^0 mass and resolutions of data and MC simulation are in agreement with each other. This systematic uncertainty is therefore deemed negligible.

The systematic uncertainties due to the mixing MC model are assigned by varying the fractions of various signal components by $\pm 1\sigma$ of the quoted BFs, when available; and by one quarter of the component fraction for each unmeasured processes. The largest changes of the signal efficiencies are assigned as the corresponding systematic uncertainties, which are 1.8%, 2.6%, and

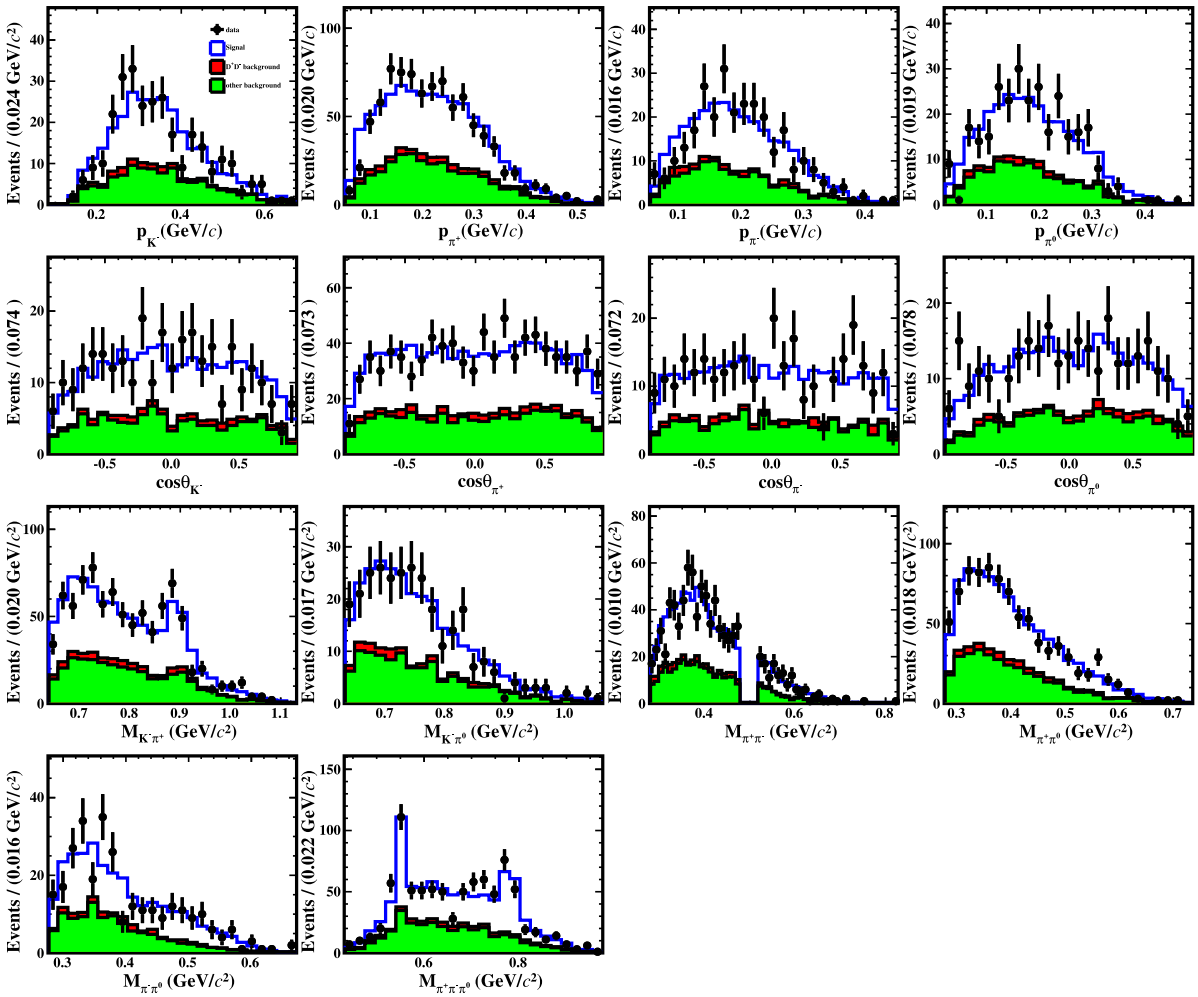

FIG. 6. Comparisons of the distributions of momenta and cosines of polar angles of daughter particles, and the invariant masses of two-body or three-body particle combinations of the accepted candidates for $D^+ \to K^-3\pi^+\pi^-\pi^0$ between data (dots with error bars) and the total MC simulation (blue histogram). This total MC histogram is the sum of the signal MC events (white histogram) plus the MC-simulated backgrounds from the inclusive MC samples (red and green histograms). Events here satisfy the additional requirements of $|M_{\rm BC}^{\rm tag} - 1.869| < 0.005$ GeV/c^2 and $|M_{\rm BC}^{\rm sig} - 1.869| < 0.005$ GeV/c^2 and there are three entries for π^+ per event.

TABLE III. Relative systematic uncertainties in % for the BF measurements.

Source	$D^0 \to K^-3\pi^+2\pi^-$	$D^0 \to K^-2\pi^+\pi^-2\pi^0$	$D^+ \to K^-3\pi^+\pi^-\pi^0$
$N_{\rm ST}^{\rm tot}$	0.3	0.3	0.3
$K^-, \pi^\pm$ tracking	3.0	2.0	2.5
$K^-, \pi^\pm$ PID	3.0	2.0	2.5
π^0 reconstruction	⋯	4.0	2.0
$\Delta E_{\rm sig}$ cut	1.5	3.6	1.6
K_S^0 rejection	Negligible	Negligible	Negligible
MC generator	1.8	2.6	1.2
MC statistics	1.1	1.6	1.3
π^0 $\mathcal{B}$	⋯	0.06	0.03
2D fit	3.5	3.5	1.5
Total	6.1	7.7	5.0

TABLE IV. Comparison of the newly measured BFs and the one previous result; the first and second uncertainties are statistical and systematic, respectively.

Signal decay	$\mathcal{B}_{\rm sig}(\times 10^{-4})$	$\mathcal{B}_{\rm FOCUS}(\times 10^{-4})$
$D^0 \to K^-3\pi^+2\pi^-$	$1.35 \pm 0.23 \pm 0.08$	$2.2 \pm 0.5 \pm 0.3$
$D^0 \to K^-2\pi^+\pi^-2\pi^0$	$19.0 \pm 1.1 \pm 1.5$	...
$D^+ \to K^-3\pi^+\pi^-\pi^0$	$6.57 \pm 0.69 \pm 0.33$	...

1.2% for $D^0 \to K^-3\pi^+2\pi^-$, $D^0 \to K^-2\pi^+\pi^-2\pi^0$ and $D^+ \to K^-3\pi^+\pi^-\pi^0$, respectively.

The uncertainties due to MC statistics, which are 1.1%, 1.6%, and 1.3% for $D^0 \to K^-3\pi^+2\pi^-$, $D^0 \to K^-2\pi^+\pi^-2\pi^0$ and $D^+ \to K^-3\pi^+\pi^-\pi^0$, respectively, are taken as individual systematic uncertainties.

The uncertainty of the quoted BF of $\pi^0 \to \gamma\gamma$ is 0.03% per π^0 [10].

The systematic uncertainty in the 2D fit to the $M_{\rm BC}^{\rm tag}$ versus $M_{\rm BC}^{\rm sig}$ distribution is examined in two ways. An alternative signal shape is obtained by varying the mean and width of the smeared Gaussian resolution function by $\pm 1\sigma$ and an alternative background shape is obtained by varying the endpoint of the ARGUS function by ± 0.2 MeV/c^2. Adding the largest effect from each pair of plus-minus variations in quadrature gives the systematic uncertainties, which are 3.5%, 3.5%, and 1.5% for $D^0 \to K^-3\pi^+2\pi^-$, $D^0 \to K^-2\pi^+\pi^-2\pi^0$ and $D^+ \to K^-3\pi^+\pi^-\pi^0$, respectively.

Table III summarizes these systematic uncertainties in the BF measurements. For each signal decay, the total systematic uncertainty is calculated by adding all above sources in quadrature; and they are 6.1%, 7.6%, and 4.9% for $D^0 \to K^-3\pi^+2\pi^-$, $D^0 \to K^-2\pi^+\pi^-2\pi^0$ and $D^+ \to K^-3\pi^+\pi^-\pi^0$, respectively.

VIII. SUMMARY

By analyzing 7.9 fb^{-1} of e^+e^- collision data taken with the BESIII detector at $E_{\rm cm} = 3.773$ GeV, we report the first observations of the hadronic decays $D^0 \to K^-2\pi^+\pi^-2\pi^0$ and $D^+ \to K^-3\pi^+\pi^-\pi^0$ as well as an improved measurement of $D^0 \to K^-3\pi^+2\pi^-$. Their absolute BFs are determined to be $\mathcal{B}(D^0 \to K^-3\pi^+2\pi^-) = (1.35 \pm 0.23 \pm 0.08) \times 10^{-4}$, $\mathcal{B}(D^0 \to K^-2\pi^+\pi^-2\pi^0) = (19.0 \pm 1.1 \pm 1.5) \times 10^{-4}$, and $\mathcal{B}(D^+ \to K^-3\pi^+\pi^-\pi^0) = (6.57 \pm 0.69 \pm 0.33) \times 10^{-4}$, where the first uncertainties are statistical and the second systematic. A summary of the measured BFs and the one previous result is shown in Table IV. In the near future, amplitude analyses of these decays with a larger data sample from BESIII [29,30] will allow exploration of the intermediate states in these decays, which benefit the understanding of the decay mechanisms of charmed mesons.

ACKNOWLEDGMENTS

The BESIII Collaboration thanks the staff of BEPCII and the IHEP computing center for their strong support. This work is supported in part by National Key R&D Program of China under Contract No. 2023YFA1606000; National Natural Science Foundation of China (NSFC) under Contracts No. 11635010, No. 11735014, No. 11935015, No. 11935016, No. 11935018, No. 12025502, No. 12035009, No. 12035013, No. 12061131003, No. 12192260, No. 12192261, No. 12192262, No. 12192263, No. 12192264, No. 12192265, No. 12221005, No. 12225509, No. 12235017, No. 12361141819; the Chinese Academy of Sciences (CAS) Large-Scale Scientific Facility Program; the CAS Center for Excellence in Particle Physics (CCEPP); Joint Large-Scale Scientific Facility Funds of the NSFC and CAS under Contract No. U1932102 and No. U1832207; CAS under Contract No. YSBR-101; 100 Talents Program of CAS; The Institute of Nuclear and Particle Physics (INPAC) and Shanghai Key Laboratory for Particle Physics and Cosmology; Agencia Nacional de InvestigaciÃn y Desarrollo de Chile (ANID), Chile under Contract No. ANID PIA/APOYO AFB230003; German Research Foundation DFG under Contract No. FOR5327; Istituto Nazionale di Fisica Nucleare, Italy; Knut and Alice Wallenberg Foundation under Contracts No. 2021.0174, No. 2021.0299; Ministry of Development of Turkey under Contract No. DPT2006K-120470; National Research Foundation of Korea under Contract No. NRF-2022R1A2C1092335; National Science and Technology fund of Mongolia; National Science Research and Innovation Fund (NSRF) via the Program Management Unit for Human Resources & Institutional Development, Research and Innovation of Thailand under Contract No. B50G670107; Polish National Science Centre under Contract No. 2019/35/O/ST2/02907; Swedish Research Council under Contract No. 2019.04595; The Swedish Foundation for International Cooperation in Research and Higher Education under Contract No. CH2018-7756; U.S. Department of Energy under Contract No. DE-FG02-05ER41374.

DATA AVAILABILITY

The data that support the findings of this article are not publicly available because of legal restrictions preventing unrestricted public distribution. The data are available from the authors upon reasonable request.

[1] H. Y. Cheng and C. W. Chiang, Phys. Rev. D **81**, 074021 (2010).
[2] Q. Qin, H. N. Li, C. D. Lü, and F. S. Yu, Phys. Rev. D **89**, 054006 (2014).
[3] H. N. Li, C. D. Lü, and F. S. Yu, Phys. Rev. D **86**, 036012 (2012).
[4] H. Y. Cheng, Phys. Rev. D **67**, 034024 (2003); **67**, 094007 (2003); **68**, 014015 (2003).
[5] P. F. Guo, D. Wang, and F. S. Yu, Nucl. Phys. Rev. **36**, 125 (2019).
[6] E. Kou *et al.* (Belle II Collaboration), Prog. Theor. Exp. Phys. **2019**, 123C01 (2019).
[7] R. Aaij *et al.* (LHCb Collaboration), arXiv:1808.08865.
[8] M. Ablikim *et al.* (BESIII Collaboration), Phys. Rev. D **107**, 032002 (2023).
[9] M. Peshkin and J. L. Rosner, Nucl. Phys. **B122**, 144 (1977).
[10] S. Navas *et al.* (Particle Data Group), Phys. Rev. D **110**, 030001 (2024).
[11] J. M. Link *et al.* (FOCUS Collaboration), Phys. Lett. B **586**, 21 (2004).
[12] M. Ablikim *et al.* (BESIII Collaboration), Chin. Phys. C **37**, 123001 (2013).
[13] M. Ablikim *et al.* (BESIII Collaboration), Phys. Lett. B **753**, 629 (2016).
[14] M. Ablikim *et al.* (BESIII Collaboration), Chin. Phys. C **48**, 123001 (2024).
[15] M. Ablikim *et al.* (BESIII Collaboration), Nucl. Instrum. Methods Phys. Res., Sect. A **614**, 345 (2010).
[16] C. H. Yu *et al.*, *Proceedings of IPAC2016, Busan, Korea* (2016).
[17] X. Li *et al.*, Radiat. Detect. Technol. Methods **1**, 13 (2017); Y. X. Guo *et al.*, Radiat. Detect. Technol. Methods **1**, 15 (2017);P. Cao *et al.*, Nucl. Instrum. Methods Phys. Res., Sect. A **953**, 163053 (2020).
[18] S. Agostinelli *et al.* (GEANT4 Collaboration), Nucl. Instrum. Methods Phys. Res., Sect. A **506**, 250 (2003).
[19] S. Jadach, B. F. L. Ward, and Z. Was, Phys. Rev. D **63**, 113009 (2001); Comput. Phys. Commun. **130**, 260 (2000).
[20] D. J. Lange, Nucl. Instrum. Methods Phys. Res., Sect. A **462**, 152 (2001); R. G. Ping, Chin. Phys. C **32**, 599 (2008).
[21] J. C. Chen, G. S. Huang, X. R. Qi, D. H. Zhang, and Y. S. Zhu, Phys. Rev. D **62**, 034003 (2000); R. L. Yang, R. G. Ping, and H. Chen, Chin. Phys. Lett. **31**, 061301 (2014).
[22] E. Barberio, B. van Eijk, and Z. Was, Comput. Phys. Commun. **66**, 115 (1991).
[23] R. M. Baltrusaitis *et al.* (MARK-III Collaboration), Phys. Rev. Lett. **56**, 2140 (1986); J. Adler *et al.* (MARK-III Collaboration), Phys. Rev. Lett. **60**, 89 (1988).
[24] K. L. He *et al.*, Proc. Sci., ACAT2007 (**2007**) 038.
[25] M. Ablikim *et al.* (BESIII Collaboration), Phys. Lett. B **734**, 227 (2014).
[26] M. Ablikim *et al.* (BESIII Collaboration), Phys. Rev. D **110**, 112006 (2024).
[27] H. Albrecht *et al.* (ARGUS Collaboration), Phys. Lett. B **241**, 278 (1990).
[28] S. Dobbs *et al.* (CLEO Collaboration), Phys. Rev. D **76**, 112001 (2007).
[29] M. Ablikim *et al.* (BESIII Collaboration), Chin. Phys. C **44**, 040001 (2020).
[30] H. B. Li and X. R. Lyu (BESIII Collaboration), Natl. Sci. Rev. **8**, 6381732 (2021).

M. Ablikim,[1] M. N. Achasov,[4,c] P. Adlarson,[76] X. C. Ai,[81] R. Aliberti,[35] A. Amoroso,[75a,75c] Q. An,[72,58,a] Y. Bai,[57] O. Bakina,[36] Y. Ban,[46,h] H.-R. Bao,[64] V. Batozskaya,[1,44] K. Begzsuren,[32] N. Berger,[35] M. Berlowski,[44] M. Bertani,[28a] D. Bettoni,[29a] F. Bianchi,[75a,75c] E. Bianco,[75a,75c] A. Bortone,[75a,75c] I. Boyko,[36] R. A. Briere,[5] A. Brueggemann,[69] H. Cai,[77] M. H. Cai,[38,k,l] X. Cai,[1,58] A. Calcaterra,[28a] G. F. Cao,[1,64] N. Cao,[1,64] S. A. Cetin,[62a] X. Y. Chai,[46,h] J. F. Chang,[1,58] G. R. Che,[43] Y. Z. Che,[1,58,64] G. Chelkov,[36,b] C. Chen,[43] C. H. Chen,[9] Chao Chen,[55] G. Chen,[1] H. S. Chen,[1,64] H. Y. Chen,[20] M. L. Chen,[1,58,64] S. J. Chen,[42] S. L. Chen,[45] S. M. Chen,[61] T. Chen,[1,64] X. R. Chen,[31,64] X. T. Chen,[1,64] Y. B. Chen,[1,58] Y. Q. Chen,[34] Z. J. Chen,[25,i] Z. K. Chen,[59] S. K. Choi,[10] X. Chu,[12,g] G. Cibinetto,[29a] F. Cossio,[75c] J. J. Cui,[50] H. L. Dai,[1,58] J. P. Dai,[79] A. Dbeyssi,[18] R. E. de Boer,[3] D. Dedovich,[36] C. Q. Deng,[73] Z. Y. Deng,[1] A. Denig,[35] I. Denysenko,[36] M. Destefanis,[75a,75c] F. De Mori,[75a,75c] B. Ding,[67,1] X. X. Ding,[46,h] Y. Ding,[34] Y. Ding,[40] Y. X. Ding,[30] J. Dong,[1,58] L. Y. Dong,[1,64] M. Y. Dong,[1,58,64] X. Dong,[77] M. C. Du,[1] S. X. Du,[81] Y. Y. Duan,[55] Z. H. Duan,[42] P. Egorov,[36,b] G. F. Fan,[42] J. J. Fan,[19] Y. H. Fan,[45] J. Fang,[59] J. Fang,[1,58] S. S. Fang,[1,64] W. X. Fang,[1] Y. Q. Fang,[1,58] R. Farinelli,[29a] L. Fava,[75b,75c] F. Feldbauer,[3] G. Felici,[28a] C. Q. Feng,[72,58] J. H. Feng,[59] Y. T. Feng,[72,58] M. Fritsch,[3] C. D. Fu,[1] J. L. Fu,[64] Y. W. Fu,[1,64] H. Gao,[64] X. B. Gao,[41] Y. N. Gao,[46,h] Y. N. Gao,[19] Y. Y. Gao,[30] Yang Gao,[72,58] S. Garbolino,[75c] I. Garzia,[29a,29b] P. T. Ge,[19] Z. W. Ge,[42] C. Geng,[59] E. M. Gersabeck,[68] A. Gilman,[70] K. Goetzen,[13] J. D. Gong,[34] L. Gong,[40] W. X. Gong,[1,58] W. Gradl,[35] S. Gramigna,[29a,29b] M. Greco,[75a,75c] M. H. Gu,[1,58] Y. T. Gu,[15] C. Y. Guan,[1,64] A. Q. Guo,[31] L. B. Guo,[41] M. J. Guo,[50] R. P. Guo,[49] Y. P. Guo,[12,g] A. Guskov,[36,b] J. Gutierrez,[27] K. L. Han,[64] T. T. Han,[1] F. Hanisch,[3] K. D. Hao,[72,58] X. Q. Hao,[19] F. A. Harris,[66] K. K. He,[55] K. L. He,[1,64] F. H. Heinsius,[3] C. H. Heinz,[35] Y. K. Heng,[1,58,64] C. Herold,[60] T. Holtmann,[3] P. C. Hong,[34] G. Y. Hou,[1,64] X. T. Hou,[1,64] Y. R. Hou,[64] Z. L. Hou,[1] B. Y. Hu,[59] H. M. Hu,[1,64] J. F. Hu,[56,j] Q. P. Hu,[72,58] S. L. Hu,[12,g] T. Hu,[1,58,64] Y. Hu,[1] Z. M. Hu,[59] G. S. Huang,[72,58] K. X. Huang,[59] L. Q. Huang,[31,64] P. Huang,[42] X. T. Huang,[50] Y. P. Huang,[1] Y. S. Huang,[59] T. Hussain,[74] N. Hüsken,[35] N. in der Wiesche,[69] J. Jackson,[27] S. Janchiv,[32] Q. Ji,[1] Q. P. Ji,[19]

W. Ji,[1,64] X. B. Ji,[1,64] X. L. Ji,[1,58] Y. Y. Ji,[50] Z. K. Jia,[72,58] D. Jiang,[1,64] H. B. Jiang,[77] P. C. Jiang,[46,h] S. J. Jiang,[9] T. J. Jiang,[16] X. S. Jiang,[1,58,64] Y. Jiang,[64] J. B. Jiao,[50] J. K. Jiao,[34] Z. Jiao,[23] S. Jin,[42] Y. Jin,[67] M. Q. Jing,[1,64] X. M. Jing,[64] T. Johansson,[76] S. Kabana,[33] N. Kalantar-Nayestanaki,[65] X. L. Kang,[9] X. S. Kang,[40] M. Kavatsyuk,[65] B. C. Ke,[81] V. Khachatryan,[27] A. Khoukaz,[69] R. Kiuchi,[1] O. B. Kolcu,[62a] B. Kopf,[3] M. Kuessner,[3] X. Kui,[1,64] N. Kumar,[26] A. Kupsc,[44,76] W. Kühn,[37] Q. Lan,[73] W. N. Lan,[19] T. T. Lei,[72,58] M. Lellmann,[35] T. Lenz,[35] C. Li,[43] C. Li,[47] C. H. Li,[39] C. K. Li,[20] Cheng Li,[72,58] D. M. Li,[81] F. Li,[1,58] G. Li,[1] H. B. Li,[1,64] H. J. Li,[19] H. N. Li,[56,j] Hui Li,[43] J. R. Li,[61] J. S. Li,[59] K. Li,[1] K. L. Li,[38,k,l] K. L. Li,[19] L. J. Li,[1,64] Lei Li,[48] M. H. Li,[43] M. R. Li,[1,64] P. L. Li,[64] P. R. Li,[38,k,l] Q. M. Li,[1,64] Q. X. Li,[50] R. Li,[17,31] T. Li,[50] T. Y. Li,[43] W. D. Li,[1,64] W. G. Li,[1,a] X. Li,[1,64] X. H. Li,[72,58] X. L. Li,[50] X. Y. Li,[1,8] X. Z. Li,[59] Y. Li,[19] Y. G. Li,[46,h] Y. P. Li,[34] Z. J. Li,[59] Z. Y. Li,[79] C. Liang,[42] H. Liang,[72,58] Y. F. Liang,[54] Y. T. Liang,[31,64] G. R. Liao,[14] L. B. Liao,[59] M. H. Liao,[59] Y. P. Liao,[1,64] J. Libby,[26] A. Limphirat,[60] C. C. Lin,[55] C. X. Lin,[64] D. X. Lin,[31,64] L. Q. Lin,[39] T. Lin,[1] B. J. Liu,[1] B. X. Liu,[77] C. Liu,[34] C. X. Liu,[1] F. Liu,[1] F. H. Liu,[53] Feng Liu,[6] G. M. Liu,[56,j] H. Liu,[38,k,l] H. B. Liu,[15] H. H. Liu,[1] H. M. Liu,[1,64] Huihui Liu,[21] J. B. Liu,[72,58] J. J. Liu,[20] K. Liu,[38,k,l] K. Liu,[73] K. Y. Liu,[40] Ke Liu,[22] L. Liu,[72,58] L. C. Liu,[43] Lu Liu,[43] P. L. Liu,[1] Q. Liu,[64] S. B. Liu,[72,58] T. Liu,[12,g] W. K. Liu,[43] W. M. Liu,[72,58] W. T. Liu,[39] X. Liu,[38,k,l] X. Liu,[39] X. Y. Liu,[77] Y. Liu,[38,k,l] Y. Liu,[81] Y. Liu,[81] Y. B. Liu,[43] Z. A. Liu,[1,58,64] Z. D. Liu,[9] Z. Q. Liu,[50] X. C. Lou,[1,58,64] F. X. Lu,[59] H. J. Lu,[23] J. G. Lu,[1,58] Y. Lu,[7] Y. H. Lu,[1,64] Y. P. Lu,[1,58] Z. H. Lu,[1,64] C. L. Luo,[41] J. R. Luo,[59] J. S. Luo,[1,64] M. X. Luo,[80] T. Luo,[12,g] X. L. Luo,[1,58] Z. Y. Lv,[22] X. R. Lyu,[64,p] Y. F. Lyu,[43] Y. H. Lyu,[81] F. C. Ma,[40] H. Ma,[79] H. L. Ma,[1] J. L. Ma,[1,64] L. L. Ma,[50] L. R. Ma,[67] Q. M. Ma,[1] R. Q. Ma,[1,64] R. Y. Ma,[19] T. Ma,[72,58] X. T. Ma,[1,64] X. Y. Ma,[1,58] Y. M. Ma,[31] F. E. Maas,[18] I. MacKay,[70] M. Maggiora,[75a,75c] S. Malde,[70] Y. J. Mao,[46,h] Z. P. Mao,[1] S. Marcello,[75a,75c] F. M. Melendi,[29a,29b] Y. H. Meng,[64] Z. X. Meng,[67] J. G. Messchendorp,[13,65] G. Mezzadri,[29a] H. Miao,[1,64] T. J. Min,[42] R. E. Mitchell,[27] X. H. Mo,[1,58,64] B. Moses,[27] N. Yu. Muchnoi,[4,c] J. Muskalla,[35] Y. Nefedov,[36] F. Nerling,[18,e] L. S. Nie,[20] I. B. Nikolaev,[4,c] Z. Ning,[1,58] S. Nisar,[11,m] Q. L. Niu,[38,k,l] W. D. Niu,[12,g] S. L. Olsen,[10,64] Q. Ouyang,[1,58,64] S. Pacetti,[28b,28c] X. Pan,[55] Y. Pan,[57] A. Pathak,[10] Y. P. Pei,[72,58] M. Pelizaeus,[3] H. P. Peng,[72,58] Y. Y. Peng,[38,k,l] K. Peters,[13,e] J. L. Ping,[41] R. G. Ping,[1,64] S. Plura,[35] V. Prasad,[33] F. Z. Qi,[1] H. R. Qi,[61] M. Qi,[42] S. Qian,[1,58] W. B. Qian,[64] C. F. Qiao,[64] J. H. Qiao,[19] J. J. Qin,[73] J. L. Qin,[55] L. Q. Qin,[14] L. Y. Qin,[72,58] P. B. Qin,[73] X. P. Qin,[12,g] X. S. Qin,[50] Z. H. Qin,[1,58] J. F. Qiu,[1] Z. H. Qu,[73] C. F. Redmer,[35] A. Rivetti,[75c] M. Rolo,[75c] G. Rong,[1,64] S. S. Rong,[1,64] F. Rosini,[28b,28c] Ch. Rosner,[18] M. Q. Ruan,[1,58] S. N. Ruan,[43] N. Salone,[44] A. Sarantsev,[36,d] Y. Schelhaas,[35] K. Schoenning,[76] M. Scodeggio,[29a] K. Y. Shan,[12,g] W. Shan,[24] X. Y. Shan,[72,58] Z. J. Shang,[38,k,l] J. F. Shangguan,[16] L. G. Shao,[1,64] M. Shao,[72,58] C. P. Shen,[12,g] H. F. Shen,[1,8] W. H. Shen,[64] X. Y. Shen,[1,64] B. A. Shi,[64] H. Shi,[72,58] J. L. Shi,[12,g] J. Y. Shi,[1] S. Y. Shi,[73] X. Shi,[1,58] H. L. Song,[72,58] J. J. Song,[19] T. Z. Song,[59] W. M. Song,[34,1] Y. X. Song,[46,h,n] S. Sosio,[75a,75c] S. Spataro,[75a,75c] F. Stieler,[35] S. S. Su,[40] Y. J. Su,[64] G. B. Sun,[77] G. X. Sun,[1] H. Sun,[64] H. K. Sun,[1] J. F. Sun,[19] K. Sun,[61] L. Sun,[77] S. S. Sun,[1,64] T. Sun,[51,f] Y. C. Sun,[77] Y. H. Sun,[30] Y. J. Sun,[72,58] Y. Z. Sun,[1] Z. Q. Sun,[1,64] Z. T. Sun,[50] C. J. Tang,[54] G. Y. Tang,[1] J. Tang,[59] L. F. Tang,[39] M. Tang,[72,58] Y. A. Tang,[77] L. Y. Tao,[73] M. Tat,[70] J. X. Teng,[72,58] J. Y. Tian,[72,58] W. H. Tian,[59] Y. Tian,[31] Z. F. Tian,[77] I. Uman,[62b] B. Wang,[59] B. Wang,[1] Bo Wang,[72,58] C. Wang,[19] Cong Wang,[22] D. Y. Wang,[46,h] H. J. Wang,[38,k,l] J. J. Wang,[77] K. Wang,[1,58] L. L. Wang,[1] L. W. Wang,[34] M. Wang,[50] M. Wang,[72,58] N. Y. Wang,[64] S. Wang,[12,g] T. Wang,[12,g] T. J. Wang,[43] W. Wang,[73] W. Wang,[59] W. P. Wang,[35,58,72,o] X. Wang,[46,h] X. F. Wang,[38,k,l] X. J. Wang,[39] X. L. Wang,[12,g] X. N. Wang,[1] Y. Wang,[61] Y. D. Wang,[45] Y. F. Wang,[1,58,64] Y. H. Wang,[38,k,l] Y. L. Wang,[19] Y. N. Wang,[77] Y. Q. Wang,[1] Yaqian Wang,[17] Yi Wang,[61] Yuan Wang,[17,31] Z. Wang,[1,58] Z. L. Wang,[73] Z. L. Wang,[2] Z. Q. Wang,[12,g] Z. Y. Wang,[1,64] D. H. Wei,[14] H. R. Wei,[43] F. Weidner,[69] S. P. Wen,[1] Y. R. Wen,[39] U. Wiedner,[3] G. Wilkinson,[70] M. Wolke,[76] C. Wu,[39] J. F. Wu,[1,8] L. H. Wu,[1] L. J. Wu,[1,64] Lianjie Wu,[19] S. G. Wu,[1,64] S. M. Wu,[64] X. Wu,[12,g] X. H. Wu,[34] Y. J. Wu,[31] Z. Wu,[1,58] L. Xia,[72,58] X. M. Xian,[39] B. H. Xiang,[1,64] T. Xiang,[46,h] D. Xiao,[38,k,l] G. Y. Xiao,[42] H. Xiao,[73] Y. L. Xiao,[12,g] Z. J. Xiao,[41] C. Xie,[42] K. J. Xie,[1,64] X. H. Xie,[46,h] Y. Xie,[50] Y. G. Xie,[1,58] Y. H. Xie,[6] Z. P. Xie,[72,58] T. Y. Xing,[1,64] C. F. Xu,[1,64] C. J. Xu,[59] G. F. Xu,[1] H. Y. Xu,[2] H. Y. Xu,[67,2] M. Xu,[72,58] Q. J. Xu,[16] Q. N. Xu,[30] W. L. Xu,[67] X. P. Xu,[55] Y. Xu,[40] Y. Xu,[12,g] Y. C. Xu,[78] Z. S. Xu,[64] H. Y. Yan,[39] L. Yan,[12,g] W. B. Yan,[72,58] W. C. Yan,[81] W. P. Yan,[19] X. Q. Yan,[1,64] H. J. Yang,[51,f] H. L. Yang,[34] H. X. Yang,[1] J. H. Yang,[42] R. J. Yang,[19] T. Yang,[1] Y. Yang,[12,g] Y. F. Yang,[43] Y. H. Yang,[42] Y. Q. Yang,[9] Y. X. Yang,[1,64] Y. Z. Yang,[19] M. Ye,[1,58] M. H. Ye,[8] Junhao Yin,[43] Z. Y. You,[59] B. X. Yu,[1,58,64] C. X. Yu,[43] G. Yu,[13] J. S. Yu,[25,i] M. C. Yu,[40] T. Yu,[73] X. D. Yu,[46,h] Y. C. Yu,[81] C. Z. Yuan,[1,64] H. Yuan,[1,64] J. Yuan,[45] J. Yuan,[34] L. Yuan,[2] S. C. Yuan,[1,64] Y. Yuan,[1,64] Z. Y. Yuan,[59] C. X. Yue,[39] Ying Yue,[19] A. A. Zafar,[74] S. H. Zeng,[63] X. Zeng,[12,g] Y. Zeng,[25,i] Y. J. Zeng,[1,64] Y. J. Zeng,[59] X. Y. Zhai,[34] Y. H. Zhan,[59] A. Q. Zhang,[1,64] B. L. Zhang,[1,64] B. X. Zhang,[1] D. H. Zhang,[43] G. Y. Zhang,[19] G. Y. Zhang,[1,64] H. Zhang,[72,58] H. Zhang,[81] H. C. Zhang,[1,58,64] H. H. Zhang,[59] H. Q. Zhang,[1,58,64] H. R. Zhang,[72,58] H. Y. Zhang,[1,58] J. Zhang,[59] J. Zhang,[81] J. J. Zhang,[52] J. L. Zhang,[20]

J. Q. Zhang,[41] J. S. Zhang,[12,g] J. W. Zhang,[1,58,64] J. X. Zhang,[38,k,l] J. Y. Zhang,[1] J. Z. Zhang,[1,64] Jianyu Zhang,[64] L. M. Zhang,[61] Lei Zhang,[42] N. Zhang,[81] P. Zhang,[1,64] Q. Zhang,[19] Q. Y. Zhang,[34] R. Y. Zhang,[38,k,l] S. H. Zhang,[1,64] Shulei Zhang,[25,i] X. M. Zhang,[1] X. Y. Zhang,[40] X. Y. Zhang,[50] Y. Zhang,[73] Y. Zhang,[1] Y. T. Zhang,[81] Y. H. Zhang,[1,58] Y. M. Zhang,[39] Z. D. Zhang,[1] Z. H. Zhang,[1] Z. L. Zhang,[34] Z. L. Zhang,[55] Z. X. Zhang,[19] Z. Y. Zhang,[43] Z. Y. Zhang,[77] Z. Z. Zhang,[45] Zh. Zh. Zhang,[19] G. Zhao,[1] J. Y. Zhao,[1,64] J. Z. Zhao,[1,58] L. Zhao,[1] Lei Zhao,[72,58] M. G. Zhao,[43] N. Zhao,[79] R. P. Zhao,[64] S. J. Zhao,[81] Y. B. Zhao,[1,58] Y. L. Zhao,[55] Y. X. Zhao,[31,64] Z. G. Zhao,[72,58] A. Zhemchugov,[36,b] B. Zheng,[73] B. M. Zheng,[34] J. P. Zheng,[1,58] W. J. Zheng,[1,64] X. R. Zheng,[19] Y. H. Zheng,[64,p] B. Zhong,[41] X. Zhong,[59] H. Zhou,[35,50,o] J. Q. Zhou,[34] J. Y. Zhou,[34] S. Zhou,[6] X. Zhou,[77] X. K. Zhou,[6] X. R. Zhou,[72,58] X. Y. Zhou,[39] Y. Z. Zhou,[12,g] Z. C. Zhou,[20] A. N. Zhu,[64] J. Zhu,[43] K. Zhu,[1] K. J. Zhu,[1,58,64] K. S. Zhu,[12,g] L. Zhu,[34] L. X. Zhu,[64] S. H. Zhu,[71] T. J. Zhu,[12,g] W. D. Zhu,[12,g] W. D. Zhu,[41] W. J. Zhu,[1] W. Z. Zhu,[19] Y. C. Zhu,[72,58] Z. A. Zhu,[1,64] X. Y. Zhuang,[43] J. H. Zou,[1] and J. Zu[72,58]

(BESIII Collaboration)

[1]*Institute of High Energy Physics, Beijing 100049, People's Republic of China*
[2]*Beihang University, Beijing 100191, People's Republic of China*
[3]*Bochum Ruhr-University, D-44780 Bochum, Germany*
[4]*Budker Institute of Nuclear Physics SB RAS (BINP), Novosibirsk 630090, Russia*
[5]*Carnegie Mellon University, Pittsburgh, Pennsylvania 15213, USA*
[6]*Central China Normal University, Wuhan 430079, People's Republic of China*
[7]*Central South University, Changsha 410083, People's Republic of China*
[8]*China Center of Advanced Science and Technology, Beijing 100190, People's Republic of China*
[9]*China University of Geosciences, Wuhan 430074, People's Republic of China*
[10]*Chung-Ang University, Seoul, 06974, Republic of Korea*
[11]*COMSATS University Islamabad, Lahore Campus, Defence Road, Off Raiwind Road, 54000 Lahore, Pakistan*
[12]*Fudan University, Shanghai 200433, People's Republic of China*
[13]*GSI Helmholtzcentre for Heavy Ion Research GmbH, D-64291 Darmstadt, Germany*
[14]*Guangxi Normal University, Guilin 541004, People's Republic of China*
[15]*Guangxi University, Nanning 530004, People's Republic of China*
[16]*Hangzhou Normal University, Hangzhou 310036, People's Republic of China*
[17]*Hebei University, Baoding 071002, People's Republic of China*
[18]*Helmholtz Institute Mainz, Staudinger Weg 18, D-55099 Mainz, Germany*
[19]*Henan Normal University, Xinxiang 453007, People's Republic of China*
[20]*Henan University, Kaifeng 475004, People's Republic of China*
[21]*Henan University of Science and Technology, Luoyang 471003, People's Republic of China*
[22]*Henan University of Technology, Zhengzhou 450001, People's Republic of China*
[23]*Huangshan College, Huangshan 245000, People's Republic of China*
[24]*Hunan Normal University, Changsha 410081, People's Republic of China*
[25]*Hunan University, Changsha 410082, People's Republic of China*
[26]*Indian Institute of Technology Madras, Chennai 600036, India*
[27]*Indiana University, Bloomington, Indiana 47405, USA*
[28a]*INFN Laboratori Nazionali di Frascati, I-00044, Frascati, Italy*
[28b]*INFN Sezione di Perugia, I-06100, Perugia, Italy*
[28c]*University of Perugia, I-06100, Perugia, Italy*
[29a]*INFN Sezione di Ferrara, I-44122, Ferrara, Italy*
[29b]*University of Ferrara, I-44122, Ferrara, Italy*
[30]*Inner Mongolia University, Hohhot 010021, People's Republic of China*
[31]*Institute of Modern Physics, Lanzhou 730000, People's Republic of China*
[32]*Institute of Physics and Technology, Peace Avenue 54B, Ulaanbaatar 13330, Mongolia*
[33]*Instituto de Alta Investigación, Universidad de Tarapacá, Casilla 7D, Arica 1000000, Chile*
[34]*Jilin University, Changchun 130012, People's Republic of China*
[35]*Johannes Gutenberg University of Mainz, Johann-Joachim-Becher-Weg 45, D-55099 Mainz, Germany*
[36]*Joint Institute for Nuclear Research, 141980 Dubna, Moscow region, Russia*
[37]*Justus-Liebig-Universitaet Giessen, II. Physikalisches Institut, Heinrich-Buff-Ring 16, D-35392 Giessen, Germany*
[38]*Lanzhou University, Lanzhou 730000, People's Republic of China*
[39]*Liaoning Normal University, Dalian 116029, People's Republic of China*

[40]*Liaoning University, Shenyang 110036, People's Republic of China*
[41]*Nanjing Normal University, Nanjing 210023, People's Republic of China*
[42]*Nanjing University, Nanjing 210093, People's Republic of China*
[43]*Nankai University, Tianjin 300071, People's Republic of China*
[44]*National Centre for Nuclear Research, Warsaw 02-093, Poland*
[45]*North China Electric Power University, Beijing 102206, People's Republic of China*
[46]*Peking University, Beijing 100871, People's Republic of China*
[47]*Qufu Normal University, Qufu 273165, People's Republic of China*
[48]*Renmin University of China, Beijing 100872, People's Republic of China*
[49]*Shandong Normal University, Jinan 250014, People's Republic of China*
[50]*Shandong University, Jinan 250100, People's Republic of China*
[51]*Shanghai Jiao Tong University, Shanghai 200240, People's Republic of China*
[52]*Shanxi Normal University, Linfen 041004, People's Republic of China*
[53]*Shanxi University, Taiyuan 030006, People's Republic of China*
[54]*Sichuan University, Chengdu 610064, People's Republic of China*
[55]*Soochow University, Suzhou 215006, People's Republic of China*
[56]*South China Normal University, Guangzhou 510006, People's Republic of China*
[57]*Southeast University, Nanjing 211100, People's Republic of China*
[58]*State Key Laboratory of Particle Detection and Electronics, Beijing 100049, Hefei 230026, People's Republic of China*
[59]*Sun Yat-Sen University, Guangzhou 510275, People's Republic of China*
[60]*Suranaree University of Technology, University Avenue 111, Nakhon Ratchasima 30000, Thailand*
[61]*Tsinghua University, Beijing 100084, People's Republic of China*
[62a]*Turkish Accelerator Center Particle Factory Group, Istinye University, 34010, Istanbul, Turkey*
[62b]*Near East University, Nicosia, North Cyprus, 99138, Mersin 10, Turkey*
[63]*University of Bristol, H H Wills Physics Laboratory, Tyndall Avenue, Bristol, BS8 1TL, United Kingdom*
[64]*University of Chinese Academy of Sciences, Beijing 100049, People's Republic of China*
[65]*University of Groningen, NL-9747 AA Groningen, The Netherlands*
[66]*University of Hawaii, Honolulu, Hawaii 96822, USA*
[67]*University of Jinan, Jinan 250022, People's Republic of China*
[68]*University of Manchester, Oxford Road, Manchester, M13 9PL, United Kingdom*
[69]*University of Muenster, Wilhelm-Klemm-Strasse 9, 48149 Muenster, Germany*
[70]*University of Oxford, Keble Road, Oxford OX13RH, United Kingdom*
[71]*University of Science and Technology Liaoning, Anshan 114051, People's Republic of China*
[72]*University of Science and Technology of China, Hefei 230026, People's Republic of China*
[73]*University of South China, Hengyang 421001, People's Republic of China*
[74]*University of the Punjab, Lahore-54590, Pakistan*
[75a]*University of Turin and INFN, University of Turin, I-10125, Turin, Italy*
[75b]*University of Eastern Piedmont, I-15121, Alessandria, Italy*
[75c]*INFN, I-10125, Turin, Italy*
[76]*Uppsala University, Box 516, SE-75120 Uppsala, Sweden*
[77]*Wuhan University, Wuhan 430072, People's Republic of China*
[78]*Yantai University, Yantai 264005, People's Republic of China*
[79]*Yunnan University, Kunming 650500, People's Republic of China*
[80]*Zhejiang University, Hangzhou 310027, People's Republic of China*
[81]*Zhengzhou University, Zhengzhou 450001, People's Republic of China*

[a]Deceased.
[b]Also at the Moscow Institute of Physics and Technology, Moscow 141700, Russia.
[c]Also at the Novosibirsk State University, Novosibirsk, 630090, Russia.
[d]Also at the NRC "Kurchatov Institute", PNPI, 188300, Gatchina, Russia.
[e]Also at Goethe University Frankfurt, 60323 Frankfurt am Main, Germany.
[f]Also at Key Laboratory for Particle Physics, Astrophysics and Cosmology, Ministry of Education; Shanghai Key Laboratory for Particle Physics and Cosmology; Institute of Nuclear and Particle Physics, Shanghai 200240, People's Republic of China.
[g]Also at Key Laboratory of Nuclear Physics and Ion-beam Application (MOE) and Institute of Modern Physics, Fudan University, Shanghai 200443, People's Republic of China.
[h]Also at State Key Laboratory of Nuclear Physics and Technology, Peking University, Beijing 100871, People's Republic of China.
[i]Also at School of Physics and Electronics, Hunan University, Changsha 410082, China.
[j]Also at Guangdong Provincial Key Laboratory of Nuclear Science, Institute of Quantum Matter, South China Normal University, Guangzhou 510006, China.

[k]Also at MOE Frontiers Science Center for Rare Isotopes, Lanzhou University, Lanzhou 730000, People's Republic of China.
[l]Also at Lanzhou Center for Theoretical Physics, Lanzhou University, Lanzhou 730000, People's Republic of China.
[m]Also at the Department of Mathematical Sciences, IBA, Karachi 75270, Pakistan.
[n]Also at Ecole Polytechnique Federale de Lausanne (EPFL), CH-1015 Lausanne, Switzerland.
[o]Also at Helmholtz Institute Mainz, Staudinger Weg 18, D-55099 Mainz, Germany.
[p]Also at Hangzhou Institute for Advanced Study, University of Chinese Academy of Sciences, Hangzhou 310024, China.